Microbial Reduction and *in situ* Product Crystallization Coupled with Biocatalyst Cultivation during the Synthesis of 6*R*-Dihydrooxoisophorone

Evelyn M. Buque-Taboada,[a,b] Adrie J. J. Straathof,[a,*] Joseph J. Heijnen,[a] Luuk A. M. van der Wielen[a]

[a] Department of Biotechnology, Delft University of Technology, Julianalaan 67, 2628 BC Delft, The Netherlands
Phone: (+31)-15-278 2330, fax: (+31)-15-278 2355, e-mail: A. J. J.Straathof@tnw.tudelft.nl
[b] Department of Chemical Engineering, University of San Carlos, Talamban, Cebu City 6000, The Philippines

Received: January 19, 2005; Accepted: March 21, 2005

Abstract: An *in situ* product crystallization procedure was developed for a crystalline product formed during microbial reduction coupled with cell cultivation. The model reaction was the asymmetric reduction of 4-oxoisophorone (OIP) by baker's yeast (*Saccharomyces cerevisiae*). Yeast cells were cultivated fed-batch to reach a maximum concentration of 30 gdw·L^{-1}. The desired product, 6*R*-dihydrooxoisophorone (DOIP), may be further reduced by baker's yeast to an unwanted by-product; thus, DOIP was removed immediately from the fermenter *via* an external crystallization loop in this procedure. The OIP reduction rate was five times higher ($\cong$0.33 mmol·gdw^{-1}·h^{-1}) as compared to the reduction rate with resting cells. OIP reduction was started when the optimum cell concentration had already been reached in the reactor because the substrate (OIP) at $\geq$55 mM concentration inhibited cell growth. An appropriate supply of glucose as carbon and energy source was necessary to support the coupled reactions involving cell growth and maintenance and product formation while avoiding formation of metabolic by-products. Final DOIP yield and selectivity were 85% and 99%, respectively, while over 100 g·L^{-1} of product was obtained in the crystallizer. The product crystals with favorable properties were readily recovered from the crystallizer. These results indicate that product crystallization is not impaired by the solutes present in the fermentation medium.

Keywords: crystallization; 6*R*-dihydrooxoisophorone; *in situ* product recovery; 4-oxoisophorone; reduction; *Saccharomyces cerevisiae*

Introduction

The range of products that can be produced by microbial biotransformation is increasing as productivity improves dramatically by metabolic and process engineering. In the latter approach, maximizing the biocatalyst concentration in the reactor and/or immediately removing inhibiting or degrading products during the process can raise bioreactor productivity. This requires cell cultivation during the process especially when the biocatalyst is not commercially or readily available and/or involves *in situ* product removal.[1,2] However, simplifying the product separation and purification steps still remains a challenge as it is the cost-limiting factor in most cases.[1] When the desired product crystallizes in the reactor, it is often redissolved using organic solvents, separated and recrystallized. If the product crystallizes during fermentation and can be separated from the cells directly, production costs might be reduced dramatically.[2,3]

In previous work,[2] it was shown that with resting cells of *Saccharomyces cerevisiae*, an *in situ* product crystallization procedure by an integrated process (Figure 1) was more efficient than the non-integrated batch and fed-batch configurations. Such an integrated process

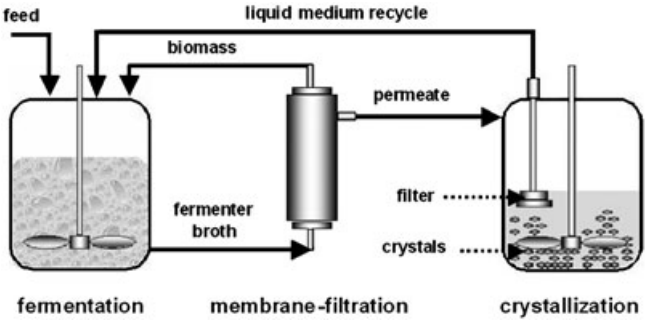

Figure 1. Schematic diagram of the integrated fermentation-crystallization process for reduction of **1**.

 DOI: 10.1002/adsc.200505024

can be improved further by implementing a close-down phase when substrate feeding is stopped and bioreduction is continued to convert all the substrate in the reactor. In various cases, the biocatalyst (micro-organism) needs to be cultivated prior to or concomitant with biotransformation and product crystallization. It would be interesting to incorporate cell growth in this *in situ* product crystallization procedure. Such an integration can possibly contribute to differences in the biotransformation and crystallization kinetics as growing cells may follow different metabolic routes compared to resting cells.

Thus, this work aims to demonstrate experimentally the impact of implementing cell cultivation concomitant with bioreduction and *in situ* product crystal formation in this integrated fermentation-crystallization process. This integration strategy should be generally applicable to processes that involve cell cultivation, biocatalytic formation of a product, and subsequent product crystallization. This approach might also be widely suitable for processes where it is required to control and reduce the product concentration in the reactor in order to prevent product toxicity, inhibition and/or degradation, and in addition, to simplify the product separation and recovery steps.

The chosen model reaction was the asymmetric reduction of 4-oxoisophorone (OIP; **1**) using baker's yeast (*S. cerevisiae*) as biocatalyst (Figure 2). The desired product is known as 6*R*-dihydrooxoisophorone (DOIP; **2**), which is a key intermediate in carotenoid synthesis[4] and in the production of saffron and tobacco flavors.[5] As baker's yeast is known to also degrade **2** mainly to 4*S*,6*R*-actinol (ACT; **3**), an unwanted by-product, product **2** must be removed from the fermenter as soon as it is formed, to prevent low product yield and selectivity. In this case, *in situ* product crystallization (ISPC) is appropriately applied.

Baker's yeast is cheap, readily available, and thus is an exceptional organism as it does not need to be cultivated

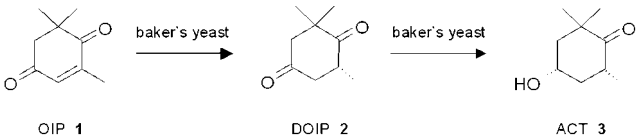

Figure 2. Model reaction: reduction of 4-oxoisophorone (**1**) by baker's yeast.

in the reactor. Still, it is an interesting case to perform reductions with pre-cultivated yeast cells. Using whole cells as biocatalyst would prove economically favorable as this allows for an easy and *in vivo* cofactor regeneration in the cell, which sustains catalytic activity for redox reactions.[6] However, aeration and nutrient feeding can be the most important constraints to consider, which can potentially complicate the whole biocatalytic process.

In this work, fed-batch cell cultivation was employed where nutrient (glucose) feed rates were varied to maximize the utilization of the carbon source and to minimize formation of metabolic by-products. Fed-batch cell cultivation was also performed concomitant with batch reduction where the initial concentrations of **1** were varied. These results were used to evaluate which conditions would better suit the subsequent integrated experiment involving *in situ* product crystallization when a close-down phase is implemented towards the end of the process.

Results and Discussion

Cell Cultivation and Batch Reduction of 1

The fed-batch cultivation of baker's yeast cells is well-established in the literature.[7] In this work, baker's yeast cultivation varied at different glucose feeding rates as

Table 1A. Biomass concentration during cell cultivation at different glucose feed rates for 24 h.

Experiment	Biomass concentration [gdw L^{-1}]		Nutrient (glucose) feed rate [mmol h^{-1}]
	Initial, C_{Xi}	Final, C_{Xf}	
$C_{m0,a}$	1.3	10.5	0.32
$C_{m1,a}$	10.6	12.5	0.31
$C_{m3,a}$	10.2	18.3	1.06
$C_{m5,a}$	10.6	37.4	1.68

Table 1B. Biomass concentration during cell cultivation and batch reduction at different glucose feed rates for 24 h.

Experiment	Biomass concentration [gdw L^{-1}]		Nutrient (glucose) feed rate [mmol h^{-1}]
	Initial, C_{Xi}	Final, C_{Xf}	
$C_{m0,b}$	0.8	5.3	0.32
$C_{m1,b}$	10.2	10.0	0.31
$C_{m3,b}$	9.8	10.2	1.06
$C_{m5,b}$	10.2	31.6	1.68

expected (see Table 1A). From an initial cell concentration $C_{Xi}=1.3$ gdw·L^{-1}, biomass accumulation in the reactor reached 10.5 gdw L^{-1} after 24 h with a glucose feed rate of 0.32 mmol h^{-1} ($C_{m0,a}$). Increasing the glucose feed concentration to over 5 times higher at 1.68 mmol h^{-1} ($C_{m5,a}$) would favor a further increase in biomass from $C_{Xi}=10.6$ gdw L^{-1} to an amount of >30 gdw L^{-1} after 24 h. This glucose feed rate can apparently support cell growth and maintenance better than the other feed rates used (i.e., $C_{m1,a}$ and $C_{m3,a}$ in Table 1A). Combining strategies involved in experiment $C_{m0,a}$ and $C_{m5,a}$ would lead to cell cultivation up to 30 gdw L^{-1} in 48 h by employing the appropriate nutrient feed rates.

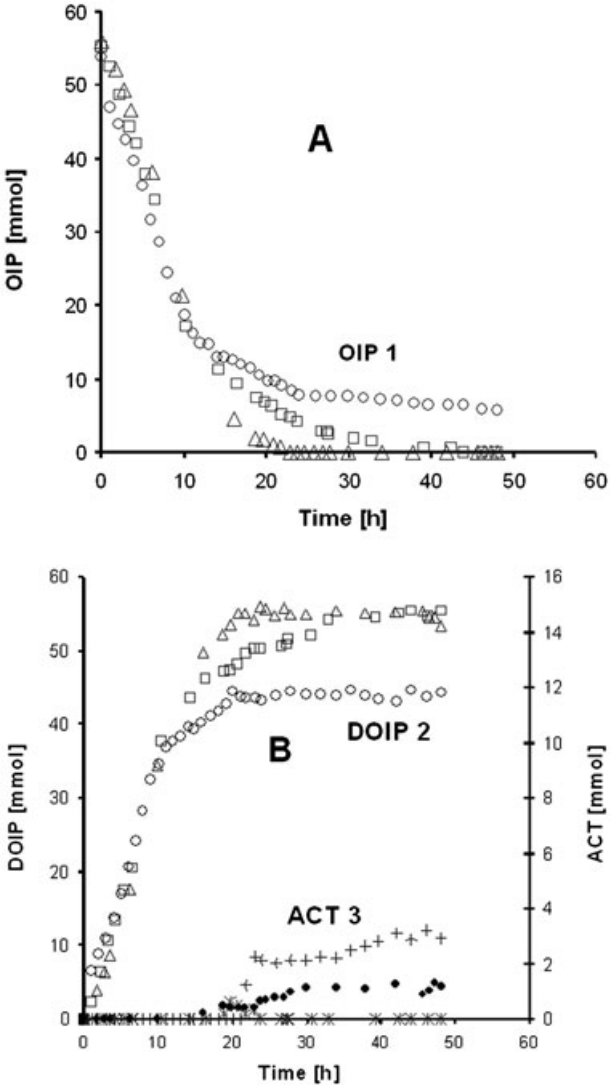

Figure 3. Total amounts of (**A**) **1** and (**B**) **2** and **3** at different nutrient feed rates during cell cultivation with simultaneous batch reduction of **1**: ○○+, C_{m1} (0.31 mmol·h^{-1}, $C_{gluc,\,feed}=$ 102.6 mM, $C_{Xi}=10.2$ gdw·L^{-1}); □□●, C_{m3} (1.06 mmol·h^{-1}, $C_{gluc,\,feed}=353.1$ mM, $C_{Xi}=9.8$ gdw·L^{-1}); △△*, C_{m5} (1.68 mmol·h^{-1}, $C_{gluc,\,feed}=560.9$ mM, $C_{Xi}=10.2$ gdw·L^{-1}).

When fed-batch cell cultivation was coupled with batch reduction of **1**, then biomass concentration in the reactor changed (Table 1B). This was obviously due to product formation, competing in the cell with cell growth and maintenance for the carbon and energy sources. The results in Table 1B show that the coupled reactions could be sustained at an approximately fivefold increase in medium nutrient feed rate ($C_{m5,b}$ at 1.68 mmol h^{-1}) when cell growth as well as bioreduction occurred simultaneously. In this case, cell accumulation in the reactor reached ≅ 30 gdw L^{-1} from an initial amount of 10.2 gdw L^{-1} (Table 1B) concomitant with batch reduction of **1** at an average biomass-specific rate of ≅ 0.33 mmol gdw^{-1} h^{-1} (Figure 3). This condition was therefore applied subsequently in the integrated fermentation-crystallization process.

The observed initial biomass-specific reduction rate of **1** of 0.33 mmol·gdw^{-1}·h^{-1} was essentially the same at different medium nutrient feed rates (Figure 3) and was about five times higher than in reductions using resting cells.[2] This suggests that metabolic reactions with growing cells can be very different as compared with resting cells, which in this case favors higher reduction capacity. Glucose as the carbon/energy source was utilized preferably for product formation rather than for cell growth as no further increase in biomass was observed when the nutrient (glucose) feed rate was <1.68 mmol·h^{-1} (Table 1B; $C_{m1,b}$ and $C_{m3,b}$). Furthermore, the final conversion rates varied; complete (100%) conversion was attained within 24 h with $C_{m5,b}$ (Figure 3), as more glucose was available for product formation and cell growth than with $C_{m1,b}$ and $C_{m3,b}$, where degrees of conversion were 85.5% and 92.2%, respectively.

At different initial concentrations of **1**, the observed initial biomass-specific reduction rates varied (Figure 4). A maximum reduction rate of 0.33 mmol·gdw^{-1}·h^{-1} was achieved at an initial concentration ($C_{OIP,i}$) of 53.8 mM (≅8.2 g·L^{-1}), but this rate decreased to 0.25 mmol·gdw^{-1}·h^{-1} and 0.23 mmol·gdw^{-1}·h^{-1} at $C_{OIP,i}=67.5$ mM (≅10.3 g·L^{-1}) and 37.2 mM (≅5.7 g·L^{-1}), respectively. This indicates that whilst batch reduction rates were much faster with growing cells than with resting cells, the maximum rate with the former was observed at a slightly lower substrate concentration ($C_{OIP,i}=55$ mM) than the latter which was at $C_{OIP,i}=$ 79 mM.[4,8] Consequently, the concentration of **1** in the reactor must be maintained (i.e., by feeding) at C_{OIP} ≅ 55 mM to implement the observed maximum reduction rate with growing cells. Towards the end of the batch reduction (see Figure 4), conversion of **1** was not complete (only 83–89%) for all experiments at the same nutrient feed rate (0.33 mmol·h^{-1}) and initial biomass concentration ($C_{Xi}=10$ gdw·L^{-1}). No biomass growth was observed in these cases; rather a slight decrease in biomass was noted at the end of the 48-h experiment. Obviously, the glucose supplied in these experiments was not suffi-

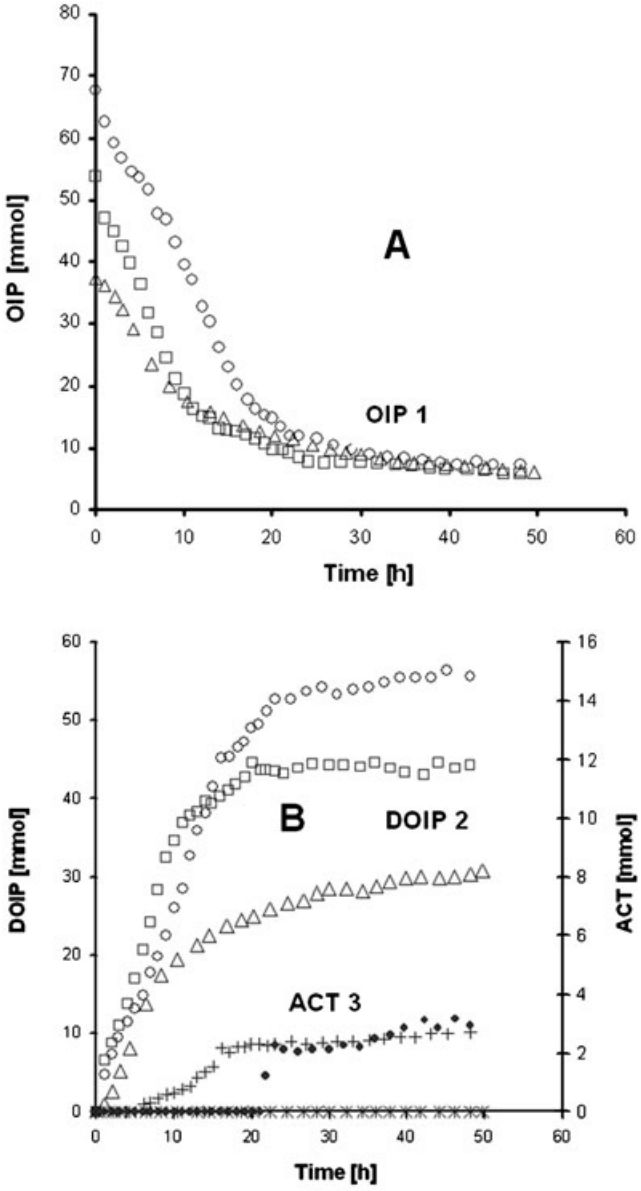

Figure 4. Total amounts of (**A**) **1** and (**B**) **2** and **3** at different initial concentrations of **1** during cell cultivation with simultaneous batch reduction: ○○+, $C_{OIP,i}=67.5$ mM; □□●, $C_{OIP,i}=53.8$ mM; △△*, $C_{OIP,i}=37.2$ mM.

cient to sustain all the required metabolic reactions in the cell.

Integrated Fermentation-Crystallization Procedure for Reduction of 1

This process was performed as shown in Figure 1 where the fermenter was attached to the crystallizer and in between the two units an ultrafiltration membrane was placed in an external loop to recycle the biomass. From the crystallizer, the mother liquor (excluding the crystals) was recirculated back to the fermenter through a 0.2-μm filter.[2] Two process schemes were designed. Process scheme **A** was an integrated fermentation-crystallization process where the reduction stage was carried out concomitant with further biomass cultivation after 24 h from the start of the experiment. Process scheme **B** was a modification of process scheme **A** where the reduction stage was implemented when the biomass concentration in the reactor had already reached an optimum level. Further elaborations of these processes are given subsequently.

Process Scheme A

This combines the cell cultivation, bioreduction and *in situ* product crystallization stages. As shown in Figure 5, the first stage of 24 h consisted of yeast cell cultivation from an initial concentration (C_{Xi}) of 1.23 gdw·L^{-1} to 9.84 gdw·L^{-1} when the glucose feed rate was 0.32 mmol·h^{-1}. In the second stage (from 24 to 48 h), reduction was started by addition of 55.5 mmol (8.4 g) **1** and feeding at 0.5 mL·h^{-1} (3.4 mmol·h^{-1}). The glucose feed rate was increased to over five-fold (1.67 mmol·h^{-1}) to further support cell growth and product formation. In the third stage, feeding of **1** was increased to 1.5 mL·h^{-1} (10.2 mmol·h^{-1}) and the glucose feed rate was raised to 6.01 mmol·h^{-1} as biomass was expected to increase to a maximum amount of about 30 gdw·L^{-1}. However, the results in Figure 5 show that biomass did not increase in stage 2 when reduction of **1** was implemented. Rather, it remained constant during this period (contrary with batch reduction when cell dry weight simultaneously increased as shown earlier). Eventually,

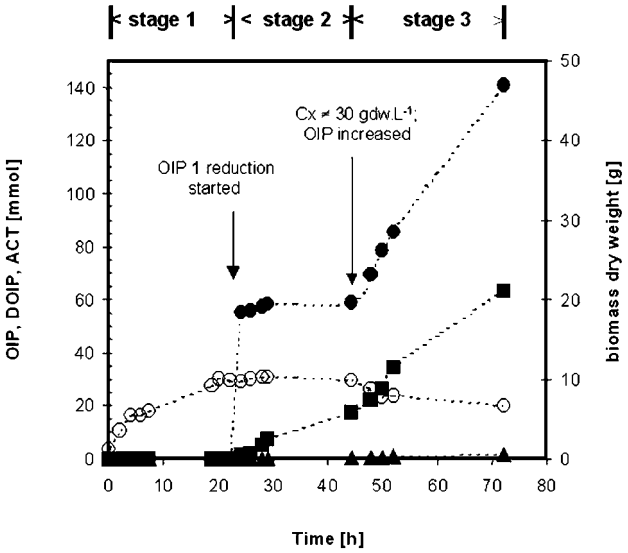

Figure 5. Process scheme **A**: Total amounts of **1** (●), **2** (■), **3** (▲) and biomass (○) in the reactor. Reduction was started after 24 h (stage 2) and no further increase in biomass was observed after this time.

it decreased in stage 3 when **1** started to accumulate in the reactor. Biomass disintegration and lysis occurred at this stage, resulting to the formation of biomass (debris) aggregates, which caused severe clogging in the ultrafiltration membrane. After 72 h, the biomass concentration (C_X) was 6.28 gdw·L^{-1}.

In this case, when **1** was fed such that its concentration was constant in the reactor (i.e., $C_{OIP} \geq 55$ mM), cell growth was inhibited as illustrated in Figure 5. The expected maximum amount of cells in the reactor was not attained. Nevertheless, reduction of **1** occurred as **2** increased in time. This indicates that the cells favored the utilization of glucose for product formation (reduction of **1**) rather than cell growth. Hence, feeding of **1** should be started at the moment that the targeted maximum biomass concentration has been reached in order to maximize bioreactor productivity.

*Process Scheme **B***

In this experiment, the observations and results obtained in process scheme **A** were considered. As shown in Figure 6, the reduction of **1** was started in stage 3 when the cell concentration in the reactor had already reached 30 gdw·L^{-1} to avoid growth inhibition and maximize bioreactor productivity. Compound **1** was added in the reactor at 56.5 mmol (8.6 g) and at the same time, fed at 1.5 mL·h^{-1} (10.2 mmol·h^{-1}) to maintain the concentration of **1** in the reactor that allows the maximum reduction rate. The glucose feed rate was also raised, to 6.04 mmol·h^{-1}, to further sustain product formation and cell maintenance. The results (Figure 6) show that the biomass concentration in the reactor was indeed maintained during reduction of **1** in stage 3 as the average biomass dry weight was 30.5 g. The concentration of **1** in the reactor was constant at $C_{OIP} \cong 60$ mM, which indicates that the feed rate of **1** (1.5 mL·h^{-1} = 10.2 mmol·h^{-1}) was equal to the observed reduction rate ($\cong$0.33 mmol·gdw^{-1}·h^{-1}). This was a favorable situation for an integrated process because the reduction rate was maximal by keeping the concentration of **1** in the reactor at a constant level while avoiding substrate inhibition and cell lysis.

At different stages during the experiment, the glucose feed rate was raised appropriately to sustain the required metabolic reactions in the cell, and support biocatalytic activity. Dissolved oxygen during the experiment was constantly above 50% of air saturation. Metabolic by-products in the samples such as ethanol and acetate were negligible.

In Table 2 are shown the important process parameters usually used to assess the efficiency of a certain biocatalytic process.[9] In this process scheme, the final yield and selectivity of **2** were 85% and 99%, respectively. The latter indicates a negligible degradation of **2**, rendering ISPC an effective method for *in situ* product removal during the integrated process. In addition to the dissolved **2**, such as shown in Figure 6 for the reactor, crystals of **2** (60.50 g) accumulated in the crystallizer and were readily recovered. Final washing with ice-cold water, filtration and drying gave product crystals of 99.5% purity. The enantiomeric excess (ee) of **2** was $\geq$ 98%, making the aforementioned procedure an attractive option for enantioselective reduction of **1**. The biocatalyst consumption rate was 0.42 kg per kg of **2** obtained; this can further be reduced when the reduction process is continued up to several days more before the close-down phase. This is a potential benefit in particular for other processes with more expensive microbial biocatalysts. The volumetric productivity was 0.55 g·L^{-1}·h^{-1} and would certainly increase when the bioreduction process would be optimally lengthened and/or the biocatalyst cultivation period reduced.

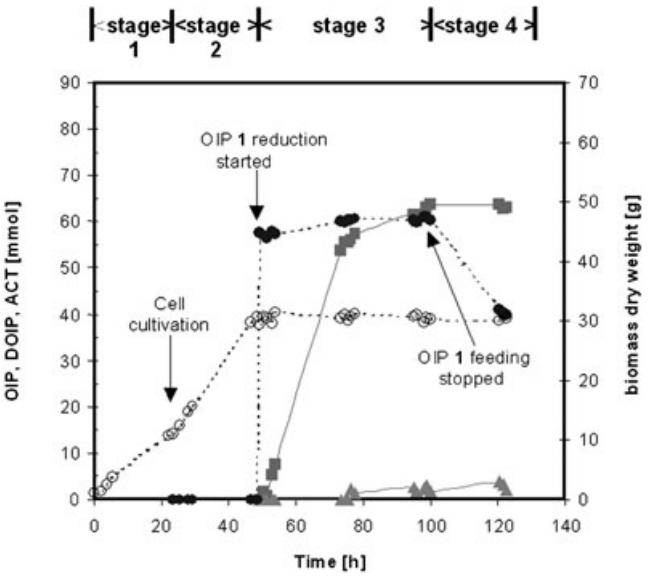

Figure 6. Process scheme **B**: Amounts of **1** (●), **2** (■), **3** (▲) and biomass (○) in the reactor. Reduction was started after 48 h (stage 3), when C_X=30 gdw·L^{-1}. Feeding of **1** was done at a rate of 1.5 mL·h^{-1}, implementing a reduction rate of about 0.33 mmol·gdw^{-1}·h^{-1} as concentration level of **1** was constant in the reactor. During the close-down phase (stage 4), feeding of **1** was stopped but reduction was continued for another 24 h.

Morphology and Crystal Size Distribution of 2

It is important to assess the morphology and crystal size distribution of the resulting product as its properties (i.e., dissolution rates, viscosity, color, shape, impurity content) have a large impact on its applications and handling.[10] The crystals of **2** obtained were white and rod-like (Figure 7A). They were mechanically quite stable and tended to form large complex aggregates (Figure 7B). The results in Figure 8 show that most of the

Table 2. Process parameters for the integrated fermentation-crystallization experiment (process scheme **B**).

Parameter [units]	Results
Final yield (**2**/**1** fed), [%]	85
Final selectivity (**2**/(**2**+**3**)), [%]	98.7
Final concentration of **2** [$g \cdot L^{-1}$]	8.98[a]/101.45[b]
Biocatalyst consumption [kg/kg **2**]	0.42
Volumetric productivity [$g \cdot L^{-1} \cdot h^{-1}$]	0.55[c]/0.92[d]

[a] In fermenter.
[b] In crystallizer.
[c] During cultivation and reduction stages.
[d] During reduction stage only.

crystals have a length range of 1–30 μm and a diameter range of 1–20 μm. Considering a crystal population of 1500, the average length and diameter were 20 and 12 μm, respectively. However, due to the tendency to form aggregates, the crystal size distribution may vary in favor of the larger particles, especially when these crystals have undergone storage. When the produced crystals underwent final washing and drying to increase the purity up to 99.5% (the same purity as that of the standard sample), the crystal morphology and size distribution were comparable. This indicates that recrystallization is not required, despite the presence of many solutes in the fermentation medium used for cell growth.

This process strategy might be applicable to many biocatalytic (e.g., reduction) systems where crystalline products are obtained. Many examples of reactions where ISPR *via* crystallization might be employed are known.[2,10a,11] Products from this process can include specialty biochemicals, pharmaceuticals, and fine chemicals such as amino acids, steroids, proteins, esters and ketones. The biocatalyst involved may range from wild-type baker's yeast (*S. cerevisiae*) or bacteria (*Escherichia coli*) to genetically engineered microorganisms. However, when microbial cultivation is necessary, substrate/product inhibition, toxicity and degradation, sufficient supply of energy and carbon sources, as well as aeration and agitation, must be taken into account during the process design, amongst others, in order to obtain an economically promising biocatalytic process.

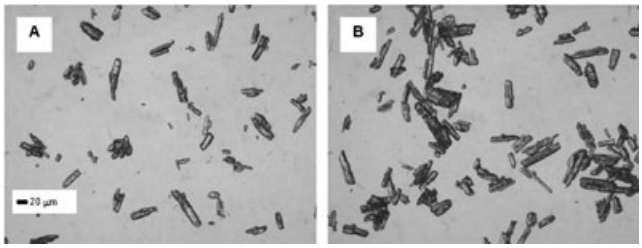

Figure 7. (**A**) Typical crystals of **2**, which are rod-like in shape, and tend to form large complex aggregates (**B**).

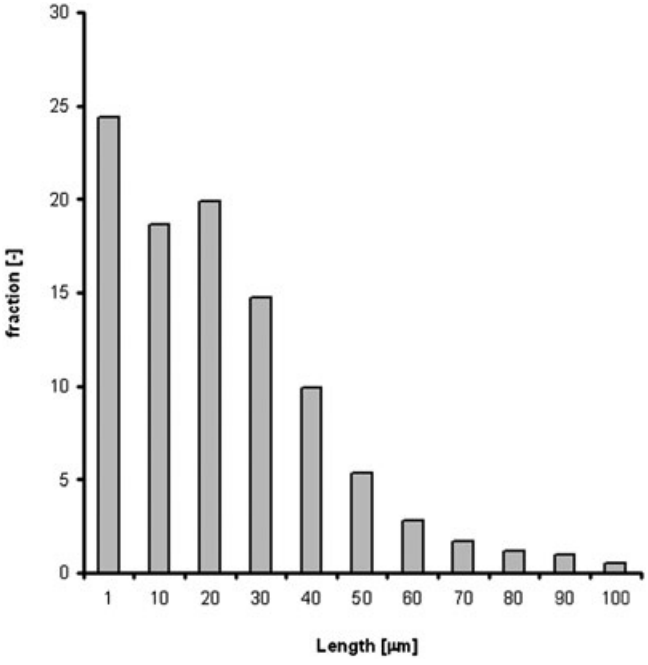

Figure 8. Crystal size distribution of **2**.

Conclusion

An efficient procedure was developed for the synthesis of **2** involving cell cultivation coupled with reduction of **1** and subsequent *in situ* product crystal formation. Process implementation is feasible, however, biocatalyst cultivation must be done prior to bioreduction and *in situ* product crystallization as **1** inhibits cell growth when its concentration in the reactor is constantly high ($\geq$ 55 mM). An appropriate supply of the carbon and energy source such as glucose is necessary as it is preferably utilized for product formation rather than cell growth. Furthermore, the reduction rate of **1** using growing cells was five times higher than using resting cells. A concentration of over 100 $g \cdot L^{-1}$ of **2** was obtained in the crystallizer at the end of the integrated experiment. The product crystals were readily recovered and did not require recrystallization.

Experimental Section

Chemicals

Compound **1** (>98%) was supplied by Fluka Biochemika (Buchs, Switzerland). Standard samples of **2** and **3** were kindly provided by DSM (Basel, Switzerland). The purity of all other chemicals used was at least laboratory grade.

Cell Cultivation and Batch Reduction of 1

Cells were cultivated aerobically in a 2-L bioreactor (Applikon, Schiedam, The Netherlands). The fermenter was equipped with two six-blade Rushton-type impellers (diameter 4.5 cm; impellers 0.5 cm above each other) and with an air outlet condenser. The total working volume was 1 L, the air flow was 0.25 vvm and the stirrer speed was 800 rpm. The temperatures of the fermenter and its attached condenser were set at 30 °C and 2–4 °C, respectively. The control of pH at 5.5 with 1 M H_2SO_4 and 2 M KOH was done *via* a biocontroller (Applikon, ADI 1010). BIOEXPERT software (Applikon, NL) was used as data-acquisition program. The parameters measured on-line during the experiment were the dissolved oxygen concentration, pH, temperature, and stirrer speed.

A mineral growth medium for baker's yeast cultivation[12] was prepared. The standard procedure was to add 0.7 L medium solution to the fermenter followed by a known amount of baker's yeast (1 g active dry baker's yeast, Fermix®; 97.5% dry weight, DSM-Gist, Delft, The Netherlands) suspended in 0.30 L medium solution to make up the 1-L total working volume. The mixture was stirred and aerated for 30 min to acclimatize (pre-incubate) the yeast. Subsequently, glucose was supplied at a rate of 0.33 mmol·h^{-1} with $C_{Gluc,\,feed} \cong 110$ mM in medium solution. Other glucose feed rates (as specified) were also used in various experiments. The reactor system was allowed 2 h to attain stationary oxygen consumption at 30 °C. Samples of the reactor liquid were analyzed for biomass dry weight and glucose concentration. Ethanol and acetate concentrations in the samples were also checked occasionally.

For batch reductions, the reaction was started by addition of a known amount in the range of 5–10 g of pure **1**, after the 2-h acclimatization period when oxygen consumption in the reactor was stabilized. For these experiments, the liquid samples were analyzed for **1**, **2** and **3** in addition to biomass dry weight and concentrations of glucose, ethanol, and acetate.

Synthesis of 2

In these experiments, the same set-up and protocols were employed as in cell cultivation and batch reductions with the following modifications. The initial cell concentration employed was about 1 gdw·L^{-1}. Glucose feed rate was varied (*as specified*) at different stages of the experiment. After 24 h, reduction was started by addition of about 8 g of pure **1** and, at the same time, **1** was fed at 0.50 mL·h^{-1} (3.4 mmol·h^{-1}) to maintain a concentration level in the reactor that avoids substrate inhibition.[4,8] The feed rate of **1** was increased to 1.5 mL·h^{-1} (10.2 mmol·h^{-1}) after 48 h as the cell concentration was expected to increase three-fold at this time. Subsequently, the integrated fermentation-crystallization procedures described previously[2] were followed. In the course of the experiment, liquid samples were taken from the reactor and the crystallizer and analyzed for **1**, **2**, and **3**. Concentrations of glucose, ethanol and acetate as well as biomass dry weight in the liquid samples from the reactor were also determined. The crystallizer volume was over 0.6 L.

Analytical Methods

Compounds **1**, **2**, and **3** in the supernatant of the reaction mixture were analyzed as described previously.[2] The enantiomeric excess (ee) of **2** was checked using a gas chromatograph (Shimadzu GC 17A) equipped with an FID and a chiral *di*Ac-*t*Bu-Si-β-cyclodextrin column (MEGA, Legnano, Italy) 25 m × 0.25 mm i.d., film thickness 0.25 μm, carrier gas helium, flow rate 0.58 mL·min^{-1}, split ratio 1:50, temperatures of injector and detector 250 °C and 280 °C, respectively. Retention times for **1**, **2**, 6*S*-dihydrooxoisophorone (6*S*-DOIP), 4*R*,6*R*-actinol, and **3** were 2.7, 5.0, 5.2, 11.1 and 11.3 min, respectively. Glucose, ethanol, acetate as well as the biomass dry weight in the reaction mixture were analyzed as described elsewhere.[13] The measured amounts of **1**, **2**, **3**, glucose and biomass were corrected for the actual volume in the reactor as well as the amounts taken out during sampling.

The product crystal morphology and the crystal size distribution (CSD) were determined using an Image Analyzer (IA) consisting of a Sony CCD video camera module (XC-77CE), an Olympus Stereo zoom microscope (SZH) and a PC with IA software LEICA Qwin version 3 (Olympus).

Acknowledgements

This research is funded by the MHO-USC-TUD Project in Chemical Engineering. We kindly thank DSM (Delft, The Netherlands) for providing baker's yeast strains and F. Hoffman-La Roche-VFCD, now DSM (Basel, Switzerland) for DOIP and actinol. We would like to thank Max Zomerdijk and Stef van Hateren (TU Delft), Victoria Napisa and her staff (USC) and Florie Gil Pino (research assistant, USC) for all the valuable support and assistance in conducting this research work.

References

[1] a) G. J. Lye, J. M. Woodley, *Trends Biotechnol.* **1999**, *17*, 395–402; b) K. Schügerl, *Biotechnol. Adv.* **2000**, *18*, 581–599; c) D. Stark, U. von Stockar, *Adv. Biochem. Eng. Biotechnol.* **2003**, *80*, 149–175; d) A. J. J. Straathof, *Biotechnol. Prog.* **2003**, *19*, 755–762.

[2] E. M. Buque-Taboada, A. J. J. Straathof, J. J. Heijnen, L. A. M. van der Wielen, *Biotechnol. Bioeng.* **2004**, *86*, 795–800.

[3] a) J. Bao, K. Koumatsu, K. Furumoto, M. Yoshimoto, K. Fukunaga, K. Nakao, *Chem. Eng. Sci.* **2001**, *56*, 6165–6170; b) J. P. Cardoso, *Biotechnol. Bioeng.* **1993**, *42*, 1068–1076; c) M. Furui, N. Sakata, O. Otsuki, T. Tosa, *Biocatalysis* **1988**, *2*, 69–77; d) S. Takamatsu, D. Y. Y. Ryu, *Biotechnol. Bioeng.* **1988**, *32*, 184–191; e) S. Takamatsu, D. Y. Y. Ryu, *Enzyme Microb. Technol.* **1988**, *10*, 593–600; f) T. Tosa, M. Furui, N. Sakata, O. Otsuki, I. Chibata, *Ann. N. Y. Acad. Sci.* **1988**, *542*, 440–443.

[4] a) H. G. W. Leuenberger, in: *Biocatalysts in Organic Synthesis*, (Eds.: J. Tramper, H. C. van der Plas, P. Linko), Elsevier Science Publishers, Amsterdam, **1985**, pp. 99–118; b) H. G. W. Leuenberger, W. Boguth, E. Widmer, R. Zell, *Helv. Chim. Acta* **1976**, *59*, 1832–1849.

[5] a) N. Hori, T. Hieda, Y. Mikami, *Agric. Biol. Chem.* **1984**, *48*, 123–129; b) K. Sode, K. Kajiwara, E. Tamiya, I. Karube, *Biocatalysis* **1987**, *1*, 77–86.
[6] a) P. D'Arrigo, G. Pedrocchi-Fantoni, S. Servi, *Adv. Appl. Microbiol.* **1997**, *44*, 81–123; b) W. F. H. Sybesma, A. J. J. Straathof, J. A. Jongejan, J. J. Heijnen, *Biocatal. Biotransform.* **1998**, *16*, 95–134.
[7] a) S. L. Chen, M. Chiger, in: *Comprehensive Biotechnology*, Vol. 3, (Ed.: M. Moo-Young), Pergamon Press, Oxford, **1985**, pp. 429–461; b) R. F. Beudeker, H. W. van-Dam, J. B. van der Plaat, K. Vellenga, in: *Yeast Biotechnology and Biocatalysis*, (Eds.: H. Verachtert and R. De Mot), Marcel Dekker, New York, **1990**, pp. 103–146; c) P. M. van Hoek, *PhD thesis*, Delft University of Technology (NL), **2000**.
[8] E. M. Buque-Taboada, A. J. J. Straathof, J. J. Heijnen, L. A. M. van der Wielen, *Enzyme Microb. Technol.* **2005**, accepted for publication.
[9] A. J. J. Straathof, S. Panke, A. Schmid, *Curr. Opin. Biotechnol.* **2002**, *13*, 548–556.
[10] a) A. McPherson, *Crystallization of Biological Macromolecules*, CSHL Press, New York, **1999**; b) J. W. Mullin, *Crystallization*, 4th edn., Butterworth-Heinemann, Oxford, **2001**; c) N. S. Tavare, *Industrial Crystallization: Process Simulation, Analysis and Design*, The Plenum Chemical Engineering Series, New York, **1995**.
[11] A. Liese, K. Seelbach, C. Wandrey, *Industrial Biotransformations*, Wiley-VCH, Weinheim, **2000**; b) R. N. Patel, *Stereoselective Biocatalysis*, Dekker, New York, **2000**.
[12] C. Herwig, U. von Stockar, *Biotechnol. Bioeng.* **2003**, *81*, 837–847.
[13] a) E. M. Buque, I. Chin-Joe, A. J. J. Straathof, J. A. Jongejan, J. J. Heijnen, *Enzyme Microb. Technol.* **2002**, *31*, 656–664; b) I. Chin-Joe, A. J. J. Straathof, J. T. Pronk, J. A. Jongejan, J. J. Heijnen, *Biotechnol. Bioeng.* **2001**, *75*, 29–38.

